Enhancing the Rate-Hardness of Haptic Interaction: Successive Force Augmentation Approach

Harsimran Singh, Dominik Janetzko, Aghil Jafari, *Member, IEEE*, Bernhard Weber, Chan-Il Lee, and Jee-Hwan Ryu, *Member, IEEE*

***Abstract*—There have been numerous approaches that have been proposed to enlarge the impedance range of haptic interaction while maintaining stability. However, enhancing the rate-hardness of haptic interaction while maintaining stability is still a challenging issue. The actual perceived rate-hardness has been much lower than what the users expect to feel. In this paper, we propose the Successive Force Augmentation (SFA) approach, which increases the impedance range by adding a feed-forward force offset to the state dependent feedback force rendered using a low stiffness value. This allows the proposed approach to display stiffness of up to 10 N/mm with Phantom Premium 1.5. It was possible to further enhance the rate-hardness by using the original value of virtual environment's stiffness for feedback force calculation during the transient response followed by normal SFA. Experimental evaluation for multi-DoF virtual environment exhibited a much higher displayed stiffness and rate-hardness compared to conventional approaches. Two user studies revealed that the increase of rate-hardness due to SFA allowed the participants to have a faster reaction time to an unexpected collision with a virtual wall and accurately discriminate between four virtual walls of different stiffness.**

***Index Terms*—Haptics and haptic interface, passivity criterion, rate-hardness, physical human-robot interaction.**

I. Introduction

ENLARGING the impedance range and increasing the rate-hardness of haptic interaction while maintaining stability has been a classical issue on the control of haptic interfaces. Lawrence et. al. [1] described rate-hardness as a tool for humans to perceive the actual hardness of the virtual environment (VE). It is the initial rate of the change of force versus velocity upon penetrating the surface. Although numerous approaches have been proposed, the actual achievable impedance and rate-hardness are still much lower than what the user perceives from real environment. Therefore, the actual implementation of haptic interaction to the wider range of applications has been severely limited.

Substantial amount of researches have been focused on increasing the impedance range of stable haptic interaction, however most of the researches have been constrained with the conventional stability methods. One of the earliest methods was putting a virtual coupling [2], but the achievable impedance was limited by the impedance of the virtual spring and damper, and it was also limited by the physical damping of the system. There were several methods proposed to increase impedance range by adding fixed amount of virtual damping. But this shifted the overall impedance range rather than increasing it. In order to inject an adaptive virtual damping, which is just enough to satisfy the time domain passivity condition in real time, Time Domain Passivity Approach (TDPA) was proposed. Even though it is known to be one of the least conservative approaches in this area, still the achievable impedance is limited.

Compared to the amount of research carried out to increase the impedance range of stable haptic interaction, not much work has been focused on enhancing its transparency. Transparency can be improved by designing or modifying the hardware of the haptic device by adapting different mechanisms. Vulliez *et al.* [3] presented a design strategy of a 6-DoF parallel haptic device, called Delhaptic, which is made by linking two Delta robots. Due to its parallel structure, it offers low inertia, high stiffness, and provides a large and singularity-free workspace, especially in rotation. Najmaei *et al.* [4] constructed a 2-DoF prototype of a haptic device which is actuated using magneto-rheological fluid clutches. This device is capable of displaying stiffness of up to 18 N/mm. Zhang *et al.* [5] demonstrated the design of a new haptic device prototype, named DentalTouch, to cope up with the challenges of having a dental simulator which can render high stiffness and low inertia. DentalTouch combines parallel and series mechanisms along with a co-actuation method to provide 3-dimensional forces, 6-DoF motions, and a stiffness range of 21 - 69 N/mm.

While some researches focus on hardware alterations, others focus on inventing new control schemes that can stabilize and

This research was partially supported by the National Research Foundation of Korea (NRF) grant funded by the Korea government (MSIP)(No. NRF- 2016R1E1A1A02921594), and by the project (Development of core teleoperation technologies for maintaining and repairing tasks in nuclear power plants) funded by the Ministry of Trade, Industry & Energy of S. Korea. *(Corresponding author: Harsimran Singh.)*

H. Singh, D. Janetzko and B. Weber are with the Institute of Robotics and Mechatronics in the German Aerospace Center (DLR), 82234 Wessling, Germany (e-mail: harsimran.singh@dlr.de; dominik.janetzko@dlr.de; bernhard.weber@dlr.de).

A. Jafari is with the Faculty of Environment and Technology, University of the West of England, Bristol, United Kingdom (e-mail: aghil.jafari@uwe.ac.uk).

Chan-Il Lee and J. H. Ryu are with the School of Mechanical Engineering, Korea University of Technology and Education, Cheonan, South Korea (e-mail: yi1128@koreatech.ac.kr; jhryu@koreatech.ac.kr)

also relieve the conservatism of conventional haptic stability control approaches. Llewellyn's stability criterion provides necessary and sufficient conditions for absolute stability of linear two-port networks [6], [7]. However, it needs to include system parameters for the controller design, which may not always be available. Jafari *et al.* [8] proposed the Input-to-state stable (ISS) approach to address the issues in absolute stability criterion in haptic interfaces. A system is known to be ISS if and only if it is dissipative. Therefore, using a control framework including a gain by considering the max slope of the input-output graph, is a sufficient condition for dissipativity, and the system becomes input-to-state stable [9]. This approach makes the output state of the system bounded. However, for some applications, this bounded behavior may be considered as unstable behavior by the operator. To address this issue an extra feed-forward gain is introduced to the controller. Still the value of the gain of this feed-forward pass is limited by noise and the application of the system. Desai *et al.* [10] presented an H_∞ based model matching framework for haptic controller design which was used to render stiff virtual walls (VW) on a Phantom Premium 1.5 haptic interface at 1 KHz. The proposed framework enabled to design controllers with increased transparency bandwidth (for a specified permissible rendering error) or minimizing the rendering error (for the desired bandwidth). The rate-hardness, however, is not the same as that of the VE. In [11] a hybrid force control algorithm employing active and passive actuators was developed to improve the stable impedance range and transparency in haptic devices. A transparency-Z-width plot was proposed as a way to evaluate the stable impedance range and transparency together. The hybrid control algorithm used parameters to share the torque demand between two actuators with a smooth transition. These parameters were determined and an artificial neural network was used to extend them to the entire achievable impedance range. However, the above mentioned proposed frameworks suffer from practical limitations because they are represented in the frequency domain and Z-domain, which may not be available online in many practical implementations. Also none of the above methods can enhance the rate-hardness [1], which is a transparency index for haptic interaction, and is more relevant than mechanical stiffness in the perception of hardness.

To overcome the aforementioned issues, this paper proposes a totally different concept of approach, which can increase the impedance range of a haptic interface along with enhancing its rate-hardness compared to other existing control methods without injecting any damping at all. We named it "Successive Force Augmentation (SFA)" approach. Although damping may stabilize the haptic interaction, but it distorts the stiffness perceived by human [12]. This study is an extension of our previous work [13], which was limited to the preliminary concept and a feasibility study. This paper fully formulates the SFA approach together with more detailed explanations, additional experimental validations, and conducts a thorough user study which manifests the feasibility of the proposed idea.

The uniqueness of SFA approach is that it takes advantage of feed-forward force that is independent of stability, while having a low enough stiffness feedback force to maintain

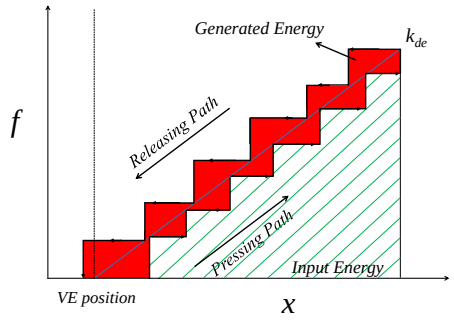

Fig. 1: Position vs. force in single contact haptic interaction.

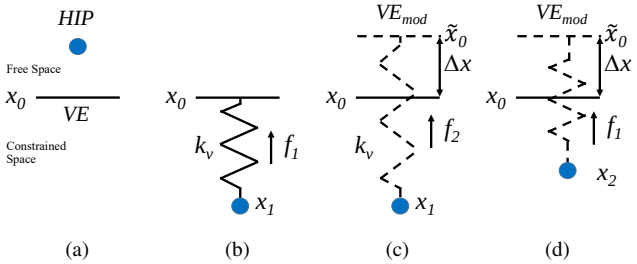

Fig. 2: Schematic diagram explaining the concept of SFA. (a) The HIP is not yet in contact with the VE, (b) Initial contact of the HIP with the VE, (c) Modifying VE's boundary-condition to increase force, (d) The HIP being pushed out of the VE due to shift in VE's boundary.

stability of the contact. The proposed SFA approach has been experimentally tested, and it is able to display stiffness of up to 10 N/mm with the Phantom Premium 1.5, which wasn't possible with any of the previously proposed methods.

II. Limitation of VE Stiffness due to Quantization

One of the major sources of non-passive behavior in haptic interfaces is the quantization effect. Fig. 1 shows the graphical representation of a single contact with a spring-like VE of stiffness k_{de}, where the system input and output variables, namely velocity and feedback force, are power conjugated, i.e. input is related to output and their product is power. In this paper, haptic interaction point (HIP) is considered to be the haptic probe position. The motion of HIP into the VE, in position vs. force plane, is termed as pressing path, and the pushing back of the HIP is termed as releasing path of the haptic interaction, as seen in Fig. 1. A single pressing and releasing path constitute an interaction cycle. The position vs. force graph shows a staircase-shaped behavior due to quantization effects. The area below the pressing line (dashed green area), can be considered the injected energy into the VE. The area below the releasing line (solid red plus dashed green area), can be considered as the energy released by the VE. Over one cycle of pressing and releasing, the released energy is larger than the injected energy, meaning that the VE generates energy which represents an active behavior. Therefore, if the actual stiffness of the VE, k_{de}, is lower than the critical stiffness (k_p), defined in [2] as follows:

$$k_p \leq \frac{2b_m}{\Delta T} \tag{1}$$

where, b_m is the physical damping of the haptic display and ΔT the sampling time, then the generated energy will be fully dissipated by the physical damping of the haptic device, therefore the effect of quantization will be eliminated and therefore the overall interaction would be stable. However, when $k_{de} > k_p$, the generated energy may not be fully dissipated by the physical damping of the device, and therefore the system may become potentially unstable. Thus, in order to maintain a stable haptic interaction the value of k_{de} should always be less than k_p.

III. Main Idea of SFA Approach

The main idea of SFA approach is shifting the boundary of VE while the HIP is in-contact with the VE. Low stiffness VE guarantees stable haptic interaction, however it limits the displayed stiffness range. By shifting the VE's boundary, we can achieve higher displayed stiffness while maintaining the same stable low stiffness. Therefore, this approach allows maintaining stable interaction while increasing transparency.

More detailed concept will be explained with schematics shown in Fig. 2. Assume that there is a ball bouncing on a floor, where the ball can be modeled as a HIP attached to a certain mass, and the floor as a VE of unilateral spring with stiffness k_v, located at x_0. At initial position (Fig. 2a) the HIP is at rest and thus has some stored potential energy (PE_{init}), because it is assumed that the HIP has some mass attached to it. Once the HIP is allowed to fall down onto the VE under the effect of gravity (Fig. 2b), the HIP penetrates the VE as long as $PE_k = PE_{init} - E_d$, where PE_k is the potential energy of the virtual spring and E_d is the energy dissipated due to the friction.

In time, the HIP would converge to a point (x_1) where the force exerted by the HIP and attached mass due to gravity in a downward direction is equal to the force of the spring in the upward direction (f_1), as depicted in Fig. 2b. At this state, if the VE is pushed upward by Δx to $\widetilde{x}_0$, while firmly holding the HIP in its position where it is still in contact with the VE(Fig. 2c), the force of the spring (f_2) would be greater than the downward force of the HIP. As a result the HIP would shift upwards, and after some transients, converge to a point x_2, where the force exerted by the HIP would be equal and opposite to that of the spring, which is again f_1.

In haptic interaction, the displayed stiffness is the interaction force from VE divided by the penetration depth. The displayed stiffness in Fig. 2d ($\frac{f_1}{x_0-x_2}$) is higher than Fig. 2b ($\frac{f_1}{x_0-x_1}$), since $|x_0-x_1| > |x_0-x_2|$. Therefore, by shifting the boundary of VE while the HIP is in-contact with the VE, we can render higher displayed stiffness although the actual stiffness of the VE stays the same.

By shifting the VE's boundary, we can display higher stiffness without actually changing the rendered stiffness. However, we need certain strategy to gradually shift the boundary in order to prevent a sudden force jump, which may cause some discontinuity. Therefore, gradual shifting with small unrecognizable steps to the operator is necessary. Interestingly, this VE boundary shifting is equivalent to adding a feed-forward force, which can be free from closed-loop stability issue. This can be seen from Fig. 2c, where the increased force f_2 is composed of spring force (f_1) and additional spring force due to shifting of VE's boundary, which is fixed and independent of state x.

$$f_2 = f_1 + k_v \Delta x \tag{2}$$

Like TDPA, the convention for force and velocity in SFA are defined such that their product is positive when power enters, and negative when power leaves the system port. Thus, the power is positive during pressing path and negative during releasing path. Therefore, the feed-forward force should only be added to the feedback force during the pressing path. This lets the SFA introduce allowable positive energy into the one-port. If additional feed-forward force is added to the feedback force during the releasing path then negative energy is added, which may increase the generated energy more than what the physical damping of the device can dissipate, thereby destabilizing the haptic interaction. The additional positive energy increases one of the power conjugate pairs, feedback force, which in turn increases the displayed stiffness. Once the displayed stiffness becomes equal to the desired stiffness, the addition of positive energy is discontinued which thereon allows the system to converge.

IV. Detailed explanation of SFA Approach

As explained in Section III, the SFA approach can be interpreted as shifting the VE's boundary while maintain a low VE stiffness, which is same as adding feed-forward offset to normal state dependent feedback force. This Section explains how this feed-forward offset is designed in order to achieve desired stiffness and reduce the performance compromise required for high stiffness stable haptic interaction. To achieve high stiffness without becoming unstable, the state dependent feedback force is rendered as:

$$f(n) = \begin{cases} k_v(x(n) - x_e(n)) + \Delta O, & \text{for } x(n) \geq x_e(n) \\ 0, & \text{for } x(n) < x_e(n) \end{cases} \tag{3}$$

where, $f(n)$ is the feedback force, k_v is the value for stiffness chosen such that $k_v < k_p$, $x_e(n)$ is the position of the VE and $x(n)$ is the position of the HIP inside the VE.

Fig. 3 graphically explains how SFA approach works at initial two subsequent interaction cycles. Once the HIP has finished its first interaction cycle, a feed-forward force offset is introduced which increases the feedback force and as a result decrease the penetration depth of the subsequent pressing path. Note that the offset is updated only at the beginning of every subsequent pressing path, and this offset is gradually increased when the displayed stiffness (k_d) is lower than the desired stiffness (k_{de})and gradually decreased when it is opposite.

$$\Delta O = \begin{cases} \Delta O + \alpha, & \text{for} \quad k_d \leq k_{de} \\ \Delta O - \alpha, & \text{for} \quad k_d > k_{de} \end{cases} \tag{4}$$
$$\text{if } (|e(n)| - |e(n-1)| > 0 \ \& \ |e(n-1)| - |e(n-2)| < 0)$$

where, $e(n) = x(n) - x_e(n)$, and α is chosen such that the slope at the beginning of each pressing path is equal to k_p rather than k_v.

$$\alpha = [x(n) - x_e(n) - x(n-1) + x_e(n-1)](k_p - k_v) \tag{5}$$

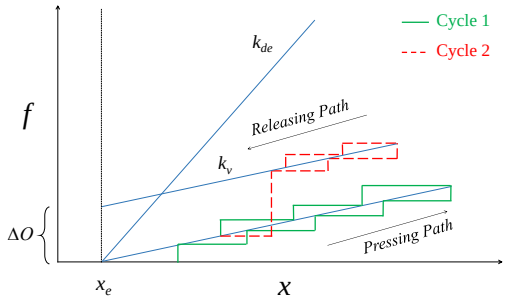

Fig. 3: Basic principle of the SFA approach.

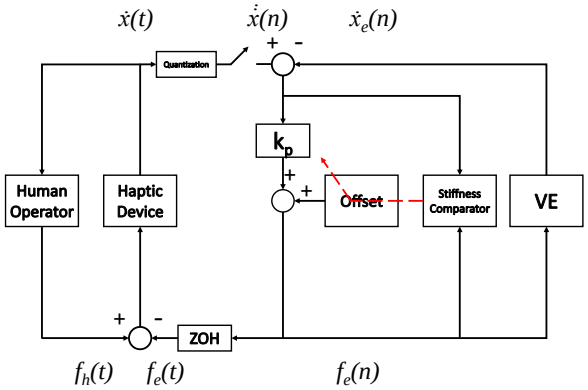

Fig. 4: Block diagram of the proposed SFA approach.

where, $x(n-1)$ and $x_e(n-1)$ are the last sampled values of position of HIP and VE, respectively. Since the value of stiffness chosen to render the VE (k_v) is smaller than the critical value k_p, therefore discretization has no effect on the haptic interface. This causes no extra generation of energy, implying that it doesn't represent an active behavior.

Fig. 4 shows the block diagram of the proposed approach. The *stiffness comparator* compares the displayed stiffness with the desired stiffness of the VE, and accordingly modifies the *offset* term only during the initial sample of every pressing path. This introduces allowable positive energy into the one-port which is added to the feedback force.

V. Experimental Evaluation of SFA Approach

A. Experimental Setup

To demonstrate the performance of the proposed approach on a impedance-type haptic display, commercially available Phantom Premium 1.5 was used. The basic specifications are: maximum force output of 8.5 N, continuous exertable force of 1.4 N, encoder resolution of 0.03 mm and a sampling rate of 1KHz. The physical damping (b_m) for which the system remains stable was selected as 0.00050 Ns/mm, therefore according to (1) the maximum stiffness of the VE for which the haptic interaction would be stable is 1 N/mm. Thus, the value of k_v in (3), which can be anything less than 1 N/mm, was experimentally selected as 0.8 N/mm. The interaction of haptic probe with a flat VE is modeled as a simple virtual spring, Fig. 8a. To calculate the interaction force between the haptic probe and the VE, a virtual proxy (VP) was introduced

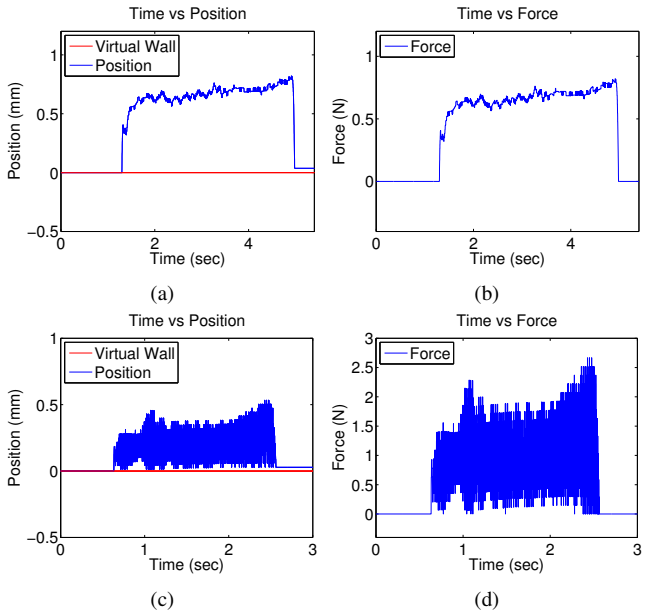

Fig. 5: (a)-(b) Stable haptic interaction with a VE of stiffness 1 N/mm, (c)-(d) Unstable haptic interaction with a VE of stiffness 5 N/mm.

that moved along the surface of the plane while having a minimum possible distance to the HIP.

B. Experimental Results and Rate-Hardness Limitation

Experimental result for when a user interacts with a flat VE having a low stiffness virtual spring, 1 N/mm, is shown in Fig. 5a and 5b. Although the system is stable, still there exists slight inherent vibrations which cannot be perceived by the user. When the stiffness was increased to 5 N/mm, the interaction became unstable, Fig. 5c and 5d. However, by implementing the SFA approach, the haptic interaction became stable even when the stiffness was increased to 10 N/mm, as shown in Fig. 6. The stiffness graph (Fig. 6c) goes on to show that the displayed stiffness approaches the desired stiffness within a few in-contact interaction cycles.

Since SFA uses low value of stiffness to render force, the rate-hardness is equal to the chosen low value of stiffness, Fig. 6d. Since k_v was chosen to be 0.8 N/mm, the initial rate of change of force versus initial velocity upon penetrating the VE is 0.8 N/mm. This gives the user a perception of touching a soft virtual surface rather than a hard one. Even though the displayed stiffness reached close to the desired stiffness within a few in-contact interaction cycles, the rate-hardness is an important factor to perceive and discriminate stiffness among objects with different hardness.

VI. Extension of SFA for Enhancing the Rate-Hardness

As shown in the previous Section, although the SFA approach can stabilize the interaction, the rate-hardness was much lower than the desired value due to the fact that the SFA approach use lower stiffness in feedback force calculation. This section extends the SFA approach to increase the rate hardness as close to the intended value of the VE stiffness.

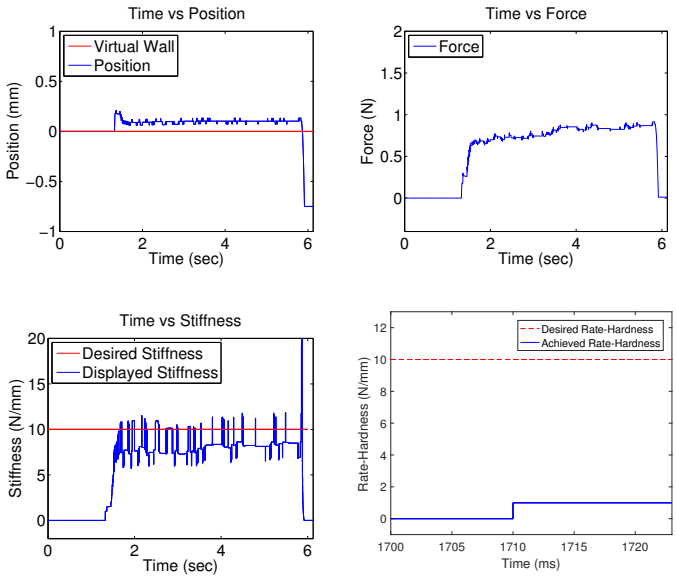

Fig. 6: Stable haptic interaction using SFA approach with a flat VE of stiffness 10 N/mm (a) Position, (b) Force, (c) Stiffness, (d) Rate-hardness.

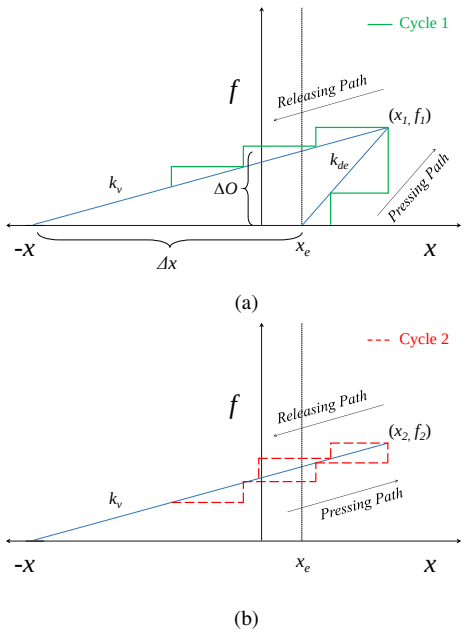

Fig. 7: Schematic diagram showing the increase of rate-hardness using extended SFA approach (a) First contact cycle, (b) Second in-contact cycle

Fig. 7 graphically shows the concept of the proposed method for making the rate-hardness equal to the desired rate-hardness of the VE. The only difference with the normal SFA approach is that the extended SFA approach follows the actual desired stiffness during the first pressing path as shown in Fig. 7a. This enhances the rate-hardness during the transient response and makes the perceived rate-hardness equal to the desired rate-hardness. Following is the force calculation scheme only for the initial contact from the free space:

if $x(n) \geq x_e(n)$ **then**
  if *Initial Pressing Path* **then**
    $f(n) = k_{de}(x(n) - x_e(n))$;
  else
    SFA
else
  $f(n) = 0$;

Perceptual hardness of the VE is closely correlated to the rate hardness, rather than with the VE's stiffness, and is given by:

$$H_R = \frac{\dot{f}(n)}{\dot{x}(n)} \tag{6}$$

where, $\dot{f}(n)$ and $\dot{x}(n)$ are the rate of change of force and velocity during the first pressing path after making contact with the VE.

After the end of the first pressing path the state dependent feedback force for the haptic interaction is rendered using (3), using a low value of stiffness, k_v. As seen in Fig. 7a, the produced energy after the end of the first interaction cycle is much greater than what can be dissipated by the device. However, most of this extra generated energy is fed back to the system again at the next pressing path as seen from Fig. 7b. If the initial contact pattern, which is using desired stiffness for pressing and lower stiffness for releasing, is repeated at every successive interaction cycle, then the interaction will go unstable due to the accumulated large amount of active energy. However, in this paper, we make the haptic interaction follow the SFA approach from second cycle onwards, which keeps the interaction stable and in-contact displayed stiffness close to the desired stiffness of the VE.

Even though the system is stable while the HIP is in-contact with the VE, but there may be an issue when the user is pulling the HIP out of the VE, where the rendered force is supposed to be set to zero. Since the feedback force for SFA is calculated using a low stiffness value followed by a feed-forward force offset, so there will be a sudden jump in force from some finite value to zero as soon as the HIP exits the VE. This sudden jump of force makes the haptic interaction jerky and gives the user an unrealistic feeling. Greater stiffness of the VE would mean a bigger offset value, which in turn would provide a greater force discontinuity.

In order to cope with this problem, we extend the releasing trajectory to the x-intercept for making a smooth force transition (see Fig. 7):

$$\widetilde{x}_{e_i} = \frac{k_v x_i - f_i}{k_v} \tag{7}$$

where, $\widetilde{x}_{e_i}$ is the shifted boundary of the VE, x_i is the penetration distance and f_i is the force after the end of i^{th} pressing path. This shifted interaction point changes after every interaction cycle. This gives the user a feeling of gradual change of force and not a sudden jerk when moving out of the VE. The small change in boundary condition is not perceived by humans owing to low position sensing resolution [14]. It

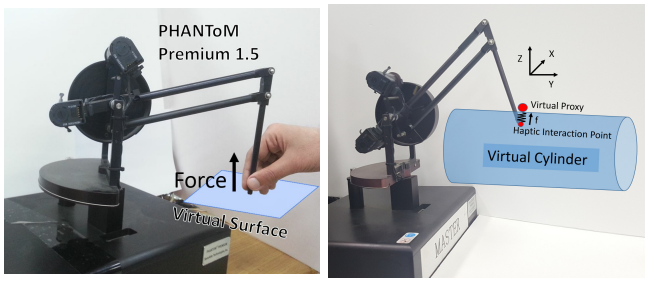

(a) (b)

Fig. 8: Phantom Premium 1.5 interacting with (a) a flat virtual surface, (b) an infinitely long virtual cylinder.

can also be inferred from (7) that smaller the value of k_v, larger will be this shift of VE's boundary.

VII. Experimental Evaluation of Extended SFA Approach

A. Experimental Setup

The same experimental setup as defined in Section V-A was used. k_v was experimentally selected to an optimal value of 0.8 N/mm. Since k_v is inversely proportional to the shift in VE's boundary (7), therefore, choosing a relatively smaller value of k_v would mean that the VE's boundary would experience a larger shift, which might be noticeable to the user. On the contrary, selecting a larger value of k_v would mean that the update of ΔO is smaller, as it is proportional to $k_p - k_v$ (5). The selection of k_v might also change depending on the k_p value of the device. Two different VE were simulated, 1) a flat surface having stiffness of 3 N/mm and 5 N/mm (Fig. 8a) and, 2) a cylinder having a radius of 6.5 cms and stiffness of 5 N/mm (Fig. 8b).

B. Experimental Results

Figs. 9 and 10 exhibit the results where a user interacts with a flat surface of stiffness 3 N/mm and 5 N/mm using the extended SFA approach. It shows that the position and force results are stable without any unwanted limit cycle oscillations. Within few interaction cycles, the displayed stiffness approaches desired stiffness of the VE. There are small vibrations present which are inherent for the device, these can also be seen in Fig. 5. Since the extended SFA approach uses the desired stiffness to render force during the initial pressing path, therefore the initial rate of change of force versus initial rate of change of velocity is equal to 3 N/mm and 5N/mm in Figs. 9 and 10 respectively. This shows that the perceived stiffness is higher for extended SFA when compared to normal SFA. When the user pulls the HIP out of the VE, it's boundary conditions are modified to eliminate any force discontinuity (7). In the experiments conducted, this shifting of boundary when interacting with a VE of 3 N/mm was 0.7 mm and when interacting with a VE of 5 N/mm was 1.2 mm. This small change in boundary condition is not perceived by human kinesthetic sense owing to low position sensing resolution [14].

For the multi-DoF scenario, the user randomly moves the haptic probe on the virtual cylinder while maintaining contact with it. The position of the haptic probe is shown in Fig. 11a along with the force response of each axis (Fig. 11b and 11c) and it's corresponding displayed stiffness (Figs. 11d and 11e). It can be seen that that force response is stable with no unwanted oscillations, implying that the user did not feel any disturbances while interacting with the virtual cylinder. The displayed stiffness for both the decoupled axis were close to desired stiffness of 5 N/mm.

One of the main reasons behind using Phantom Premium 1.5 to check the feasibility of the proposed approach, is it's low inertia and physical damping, which are least when compared to other commercially available haptic devices [15], [16]. This means that such a device is more prone to becoming unstable even with the smallest changes in external inertia (human hand) or stiffness of the VE. Also since the boundary conditions are regulated in the proposed approach, therefore devices with smaller damping tend to shift the boundary of the VE more compared to devices with higher damping. This is because b_m is inversely proportional to the shift in boundary of the VE as seen from (1) and (7). Thus if the proposed approach stabilizes Phantom Premium 1.5, then it should be able to stabilize and enhance the perceived stiffness of other commercially available haptic devices as well.

VIII. User Study

In order to examine the perceived characteristics of the system when used by a human operator, two experimental evaluations were conducted.

A. User Study 1: Contact Detection

The goal of the first study was examining whether a change in VE's stiffness, and therefore the resulting H_R, would be perceived by an operator and trigger different responses. The outcome measure was the reaction time to an unwanted collision between the HIP and a virtual structure. It was shown that the addition of haptic feedback could decrease the reaction time to a certain stimulus in comparison to mere visual feedback [17]. A decrease in reaction time for higher stiffness values, using the SFA approach, would therefore support the notion that operators could distinguish between different stiffness values.

1) Method:

Sample: The sample consisted of $N = 48$ participants (10 females; 38 males) with a mean age of 28.62 ($SD = 9.00$) years.

Apparatus: A 2 DoF, right-hand operated DLR force feedback joystick was used for the experiments [18]. The joystick is connected to a Lenovo T61p notebook which runs the VE simulation, and collects data with a sampling rate of 100 Hz (see Fig. 12).

The simulation presented virtual walls rendered with a virtual spring stiffness (k_{de}) of 2 N/mm and 4.5 N/mm, and a HIP. The two values of 2 N/mm and 4.5 N/mm were chosen to ensure better comparability to earlier research on hardness

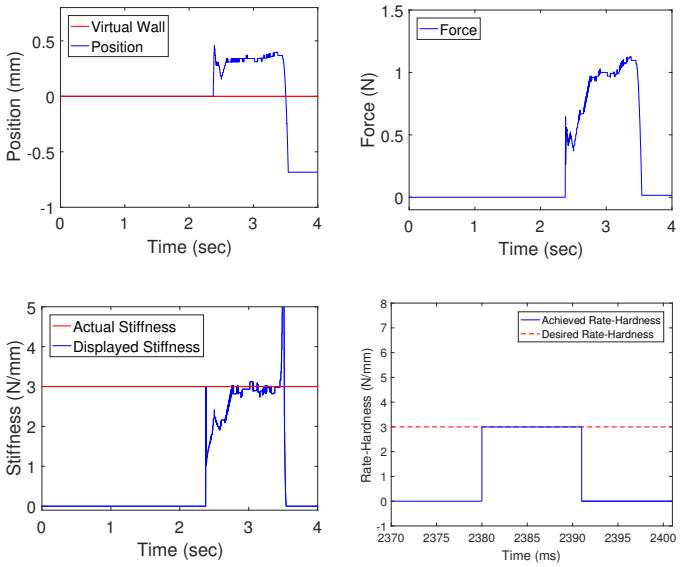

Fig. 9: Stable haptic interaction using extended SFA approach with a flat VE of stiffness 3 N/mm (a) Position, (b) Force, (c) Stiffness, (d) Rate-hardness.

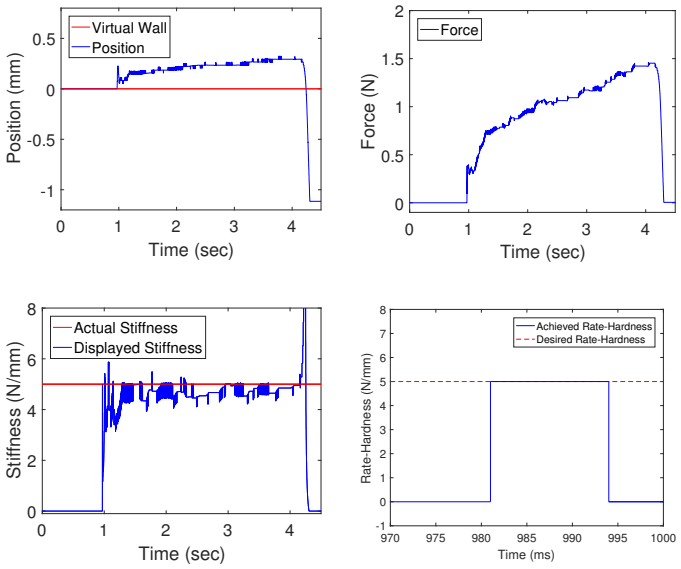

Fig. 10: Stable haptic interaction using extended SFA approach with a flat VE of stiffness 5 N/mm (a) Position, (b) Force, (c) Stiffness, (d) Rate-hardness.

perception of virtual wall contacts, e.g. conducted by [19]. In the experiment of [19], the subjective ratings on the hardness property of contacts with such virtual wall renderings were clear: For a value of 2 N/mm, the rating was lower than for the 4.5 N/mm model. However, using a value of 4.5 N/mm in comparison to a model with 7 N/mm yielded not much difference in hardness rating. It was therefore hypothesized, that in the current experiment with a similar 2-DoF force feedback joystick, the use of 2 N/mm and 4.5 N/mm should also result in difference in objective performance data with the new SFA approach.

Design: The main goal of the experiment was the examination of differences between the two k_{de} rendered by the

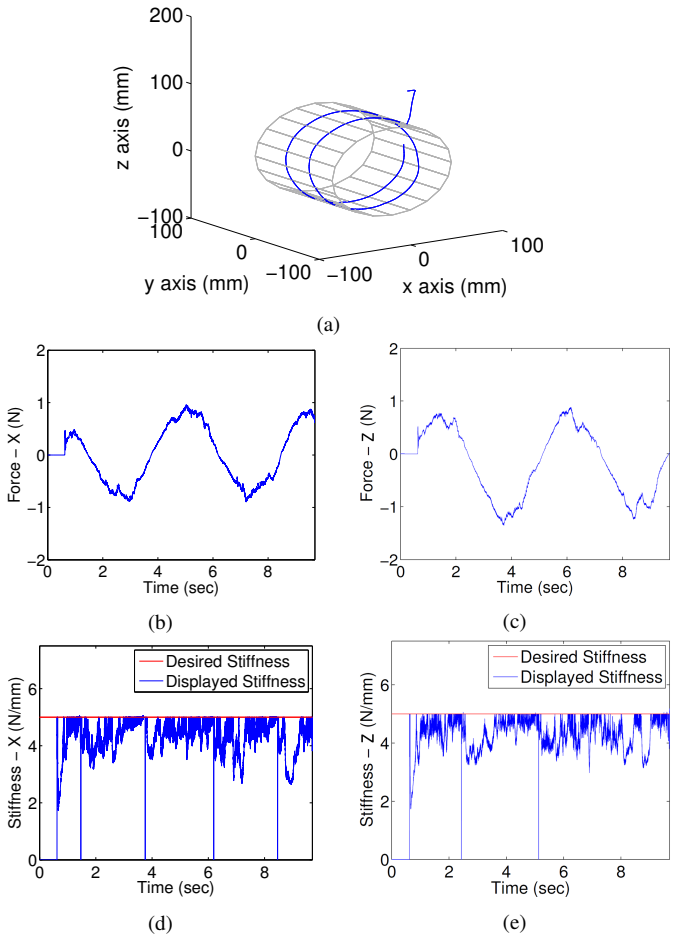

Fig. 11: Experimental results with multi-DoF SFA approach (k_x = k_z = 5 N/mm; (a) Position response, (b) Stable force response along X-axis, (c) Stable force response along Z-axis), (d) Displayed stiffness along X-axis, (e) Displayed stiffness along Z-axis

Fig. 12: Experimental setup in the first user study. The DLR force feedback joystick can be seen on the right, and the laptop simulating the VE on the left.

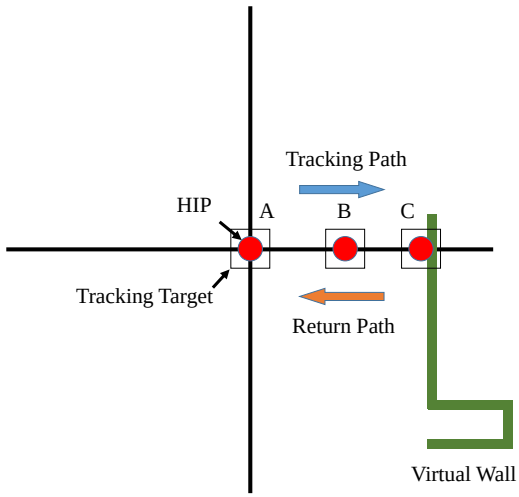

Fig. 13: Movement path in the user study. (A) Initial position of the tracking target and HIP. (B) Participants follow the tracking target on the tracking path until hitting the VW at the point of collision (C). Afterwards they would release the contact between the VW and the cursor by following the release path.

SFA approach. Users were instructed to perform a series of basic movement patterns specifically provoking a collision. A depiction of the shape of the virtual wall and the instructed movement path for the task of interest is displayed in Fig. 13. In order to rule out possible effects of the movement direction and anticipation of the distance from the VW, it was randomly positioned at eight different positions, each completed once per condition, leading to a total of eight trials per condition.

After each condition, participants were also asked to rate the information match between the position of the HIP and the feedback force generated by the SFA on a 7-point rating scale, ranging from "Not at all" to "Completely".

Task: The participants were instructed to follow a tracking target moving with constant speed until they hit the VW. This was done to achieve comparable motion speeds for all of the participants. Next, they should release the contact between the HIP and the virtual wall as fast as possible by moving in the opposite direction of the tracking path. The reaction time to the collision was measured as the time span between the first impact of the HIP on the VW and the instructed release of this contact.

2) Results: For the data analysis, five participants had to be excluded due to not being able to complete at least one of the eight trials in one or more conditions, within the alloted time frame. The number of participants for the remaining analysis was (N = 43). For these remaining participants, the reaction time measured was aggregated and averaged over the k_{de} values realized in this study. A paired t-test on the reaction time to an unplanned collision between k_{de_2} (M = 466 ms; SD = 154 ms) and $k_{de_{4.5}}$ (M = 435 ms; SD = 136 ms) revealed a statistically significant decrease in reaction time, $t(42) = 2.17$, $p < 0.05$ (Cohen's d_{paired} = 0.33; as a standardized effect size) The mean of differences between the two conditions for all the represented participants was 31 ms with a 95% confidence interval of [9; 71] ms. For the subjective rating in the information match between the position of HIP and the feedback force, no significant difference between the rating for k_{de_2} ($M = 5.21$; $SD = 1.18$) and $k_{de_{4.5}}$ ($M = 5.04$; $SD = 1.25$) could be found using a paired t-test ($t(42) = 0.98$, $p = 0.333$).

3) Discussion: The user study served as a preliminary investigation on examining whether different k_{de} are distinguishable by human operators using the extended SFA approach. The results obtained indicate that with the extended SFA approach, operators are significantly faster in reacting to an unexpected collision with a VW of higher k_{de} in comparison to a lower k_{de}. This supports the assumption, that the operators are able to discriminate between the different k_{de} values when rendered with the extended SFA approach. Interpreting this result together with the non-significant result on the subjective rating of information matching between the two k_{de}s, it should be fair to assume, that the objective performance gain was independent from a subjectively perceived change of the position of HIP. This goes on to show that the users couldn't detect a shift in the VE's boundary.

A faster reaction time for the extended SFA approach is also in line with the correlation model from [1], where, a rate-hardness difference of around 2.5 N/mm (as realized in this user study) would suggest a rate of correct hardness classification of 50%. The detection of a significant difference between the two k_{de} in this user study suggests, that with the extended SFA approach, a higher k_{de} can increase user performance above the level of just random effect. As pointed out, this study should serve as an initial proof of concept that different k_{de} rendered by extended SFA approach would actually lead to a difference in behavior for the operators.

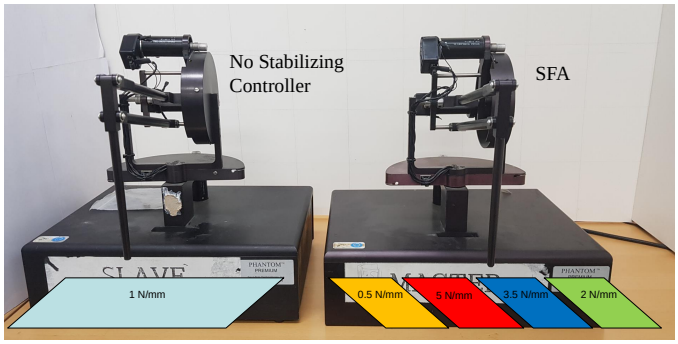

Fig. 14: Experimental setup for second user study. Phantom Premium with SFA can be seen on the right, and Phantom Premium without any stabilizing controller on the left.

B. User Study 2: Stiffness Discrimination

In addition to User Study 1, which focuses on reaction times when colliding with a VW in a 2D simulation, we conduct another study investigating 1) stiffness discrimination, and 2) detection of vibration effects, when using the SFA approach to interact with VWs of different stiffness.

1) Method:

Sample: N = 20 male subjects with an average age of 25.5 years (SD = 2.0 participated.

Apparatus: Two similar Phantom Premium 1.5 devices were placed side by side on a desk panel (see Fig. 14). The basic description of Phantom Premium 1.5 is given in Section V-A. SFA was implemented on one of the Phantom Premium 1.5 (P_{SFA}) and the other one had no stabilizing controller (P_{NC}). Four VWs of different stiffness (0.5, 2, 3.5 and 5 N/mm) were implemented side by side on P_{SFA} for the current study (see Fig. 14), which had to be discriminated by the subjects. Please note that stiffness values selected had no relation with the first user study, since the haptic devices used in both the experiments are completely different. The DLR joystick is a 2-DoF force feedback joystick whereas the Phantom Premium 1.5 is a 3-DoF low inertia impedance type device. Earlier there was no controller that could stabilize and increase the rate-hardness of a low inertia, low physical damping device, such as Phantom Premium 1.5. Thus we couldn't find any prior studies for distinction of hardness of VE such a haptic device. Therefore, for this study we selected the smallest value of stiffness (0.5 N/mm) within the stable range of the device, and the remaining 3 stiffness values were selected to be equidistant from each other. For the detection of vibration effects, another VE of stiffness 1 N/mm, which lies in the stable range of Phantom Premium 1.5, was rendered on P_{NC}. This was done to serve as a valid comparison baseline for P_{SFA}.

Experimental Task and Procedure: Participants were asked to use P_{SFA} and compare the different stiffness they felt when interacting with the four VWs. Afterwards they had to rank the different stiffness from 1 (least stiff) to 4 (most stiff) via oral feedback. The procedure was repeated four times starting with a warm-up trial and three subsequent main trials, while the respective stiffness value of each of the four VWs was randomly varied for each trial. In addition to the ranking, subjects were asked whether they had the impression that the VW's position had moved during the trial (yes/no answer format). In the vibration detection experiment, the four stiffness used in the previous experiment were sorted in a fixed, ascending order on the Phantom Premium 1.5 with SFA approach, P_{SFA}. The second Phantom Premium 1.5 without any stabilizing controller, P_{NC}, was used to compare vibrations with P_{SFA}. Participants then indicated whether they had experienced any vibration effects during the experimental trial in P_{SFA} when compared to P_{NC} (yes/no answer format).

2) Results: Comparing the actual stiffnesses with the subjects' judgments revealed a high percentage of correct rankings across all main trials (86.7-100%, see Table I: All trials). For statistical analysis of the association of actual and judged stiffness ranks, Kendall's Tau coefficient [20] was calculated. For the three main trials the correlations were r_τ (Trial 1) = 0.935, r_τ (Trial 2) = 0.951, and r_τ (Trial 3) = 0.983 and all correlations reached the level of significance (all ps < 0.001). Obviously, a learning effect occurred with almost perfect ratings after three trials (95%-100% of correct ratings). The highest stiffness configuration (5 N/mm) was correctly judged throughout the whole experiment and the lowest level of accordance was reached for second-lowest stiffness (2N/mm). No single subject had the impression that virtual walls had moved and none of them experienced any additional vibrations in P_{SFA} compared to P_{NC}.

TABLE I

All Trials		Rated Stiffness Rank			
		1	2	3	4
Actual	1	93.3%	6.67%	0%	0%
Stiffness	2	6.67%	86.7%	6.67%	0%
Rank	3	0%	6.67%	93.3%	0%
	4	0%	0%	0%	100%

3) Discussion: The quality of the presented SFA approach was evaluated in a stimulus discrimination paradigm where subjects had to distinguish and rank different stiffnesses when interacting with different VWs. In our best knowledge, there is no other hardness perception study carried out with a low inertia and damping impedance type haptic device, with VE's stiffness as high as 5 N/mm.

Results reveal that the initial accuracy level was far above guess probability (p = 0.25) for each stiffness value ranging from 0.5, 2.0 , 3.5 and 5 N/mm with very high correlations (all > 0.94) between actual and rated stiffness in the main trials. After completion of all trials, a nearly perfect accuracy rate of 95% was reached for all stiffnesses. Furthermore, we found no evidence for any disruptive and disturbing effects like perceived position drift of the VW or vibrations on P_{SFA} when compared to P_{NC}. Altogether, the findings show that the SFA generates clear and realistic forces with enhanced rate-hardness, which allows the user to distinguish between VEs of different stiffness.

IX. Conclusion

To increase the displayed stiffness and enhance the rate-hardness of impedance-type haptic interaction, this paper proposed the Successive Force Augmentation approach. The proposed approach adds allowable positive energy into the one-port in the form of feed-forward force, which is gradually modified in small unrecognizable steps. This added positive energy increases one of the power conjugate pairs, feedback force, which in turn increases the displayed stiffness. To enhance the rate-hardness, the desired stiffness of the VE is used to render feedback force only during the initial contact pressing path. Thereafter, the SFA approach guarantees stability as it uses low stiffness for rendering, which dissipates the generated energy through the inherent damping of the haptic device. This circumvents the inherent tradeoff between stability and transparency in haptic interface without limiting the feedback force or injecting additional damping into the system. Experimental evaluation was performed using Phantom Premium 1.5 where the SFA approach was implemented to render a flat virtual wall and a virtual cylinder. Results pointed out that SFA could significantly increase the displayed stiffness (up to 10 N/mm) and rate-hardness while maintaining stability. In our best knowledge there is no other approach that can display rate-hardness and displayed stiffness of 3 N/mm or greater using Phantom Premium 1.5. To show the feasibility of SFA approach, two subjective studies were performed using the DLR force feedback joystick and Phantom Premium 1.5. It revealed that (i) users had a faster reaction time to an unexpected collision with a VW of higher stiffness in comparison to a lower stiffness, and (ii) users could accurately

discriminate between four VWs of different stiffness (0.5, 2, 3.5, 5 N/mm). One can conclude that users benefited from the enhanced rate-hardness while not reporting a mismatch of information.

As a future work, further user studies, especially concerning psychophysical properties of the approach will be carried out. The SFA approach will also be extend to admittance-type haptic interface along with teleoperation system. In addition, we are planning to investigate some potential issues from multi-DOF extension of the SFA, such as how robustly the SFA can compensate the issues from rendering algorithms and how well the SFA can maintain the fidelity with more complex VE, such as sharp edges.

REFERENCES

[1] Dale Lawrence, Lucy Y Pao, Anne M Dougherty, Mark Salada, Yiannis Pavlou, et al. Rate-hardness: A new performance metric for haptic interfaces. *Robotics and Automation, IEEE Transactions on*, 16(4):357–371, 2000.

[2] J Edward Colgate, Michael C Stanley, and Justin M Brown. Issues in the haptic display of tool use. In *Intelligent Robots and Systems 95.'Human Robot Interaction and Cooperative Robots', Proceedings. 1995 IEEE/RSJ International Conference on*, volume 3, pages 140–145. IEEE, 1995.

[3] Margot Vulliez, Said Zeghloul, and Oussama Khatib. Design strategy and issues of the delthaptic, a new 6-dof parallel haptic device. *Mechanism and Machine Theory*, 128:395–411, 2018.

[4] Nima Najmaei, Ali Asadian, Mehrdad R Kermani, and Rajni V Patel. Design and performance evaluation of a prototype mrf-based haptic interface for medical applications. *IEEE/ASME Transactions on Mechatronics*, 21(1):110–121, 2016.

[5] Hongdong Zhang, Yuru Zhang, Dangxiao Wang, and Lei Lu. Dentaltouch: A haptic display with high stiffness and low inertia. In *2017 IEEE World Haptics Conference (WHC)*, pages 388–393. IEEE, 2017.

[6] Sanjit Kumar Mitra. *Analysis and synthesis of linear active networks*. John Wiley & Sons, 1969.

[7] FB Llewellyn. Some fundamental properties of transmission systems. *Proceedings of the IRE*, 40(3):271–283, 1952.

[8] A. Jafari and Jee-Hwan Ryu. Input-to-state stable approach to release the conservatism of passivity-based stable haptic interaction. In *Robotics and Automation (ICRA), 2015 IEEE International Conference on*, pages 285–290, May 2015.

[9] Abraham Jan van der Schaft and AJ Van Der Schaft. *L2-gain and passivity techniques in nonlinear control*, volume 2. Springer, 2000.

[10] Indrajit Desai, Abhishek Gupta, and Debraj Chakraborty. Rendering stiff virtual walls using model matching based haptic controller. *IEEE transactions on haptics*, 2019.

[11] Ozgur Baser, Hakan Gurocak, and E Ilhan Konukseven. Hybrid control algorithm to improve both stable impedance range and transparency in haptic devices. *Mechatronics*, 23(1):121–134, 2013.

[12] Femke E van Beek, Dennis JF Heck, Henk Nijmeijer, Wouter M Bergmann Tiest, and Astrid ML Kappers. The effect of damping on the perception of hardness. In *World Haptics Conference (WHC), 2015 IEEE*, pages 82–87. IEEE, 2015.

[13] Harsimran Singh, Aghil Jafari, and Jee-Hwan Ryu. Increasing the rate-hardness of haptic interaction: Successive force augmentation approach. In *World Haptics Conference (WHC), 2017 IEEE*, pages 653–658. IEEE, 2017.

[14] Hong Tan, J. Radcliffe, Book No. Ga, Hong Z. Tan, Brian Eberman, Mandayam A. Srinivasan, and Belinda Cheng. Human factors for the design of force-reflecting haptic interfaces, 1994.

[15] Murat Cenk Çavuşoğlu, David Feygin, and Frank Tendick. A critical study of the mechanical and electrical properties of the phantom haptic interface and improvements for highperformance control. *Presence: Teleoperators & Virtual Environments*, 11(6):555–568, 2002.

[16] Nicola Diolaiti, Günter Niemeyer, Federico Barbagli, and J Kenneth Salisbury. Stability of haptic rendering: Discretization, quantization, time delay, and coulomb effects. *IEEE Transactions on Robotics*, 22(2):256–268, 2006.

[17] Jennifer L. Burke, Matthew S. Prewett, Ashley A. Gray, Liuquin Yang, Frederick R. B. Stilson, Michael D. Coovert, Linda R. Elliot, and Elizabeth Redden. Comparing the Effects of Visual-Auditory and Visual-Tactile Feedback on User Performance: A Meta-analysis. In *Proceedings of the 8th International Conference on Multimodal Interfaces*, pages 333–338, New York, NY, 2006. ACM.

[18] Cornelia Riecke, Jordi Artigas, Ribin Balachandran, Ralph Bayer, Alexander Beyer, Bernhard Brunner, Hans Buchner, Thomas Gumpert, Robin Gruber, Franz Hacker, Klaus Landzettel, Georg Plank, Simon Schätzle, Hans-Jürgen Sedlmayr, Nikolaus Seitz, Bernhard-Michael Steinmetz, Martin Stelzer, Jörg Vogel, Bernhard Weber, Bertram Willberg, and Alin Albu-Schäffer. Kontur-2 Mission: The DLR Force Feedback Joystick for Space Telemanipulation from the ISS. In *The International Symposium on Artificial Intelligence, Robotics and Automation in Space (i-SAIRAS 2016)*, Beijing, China, 2016.

[19] L. B. Rosenberg and B. D. Adelstein. Perceptual Decomposition of Virtual Haptic Surfaces. In *Proceedings of 1993 IEEE Research Properties in Virtual Reality Symposium*, pages 46–53. IEEE Computer Society Press, 1993.

[20] Maurice G Kendall. A new measure of rank correlation. *Biometrika*, 30(1/2):81–93, 1938.